

Study of the effects of GaN buffer layer quality on the dc characteristics of AlGaIn/GaN high electron mobility transistors

Shihyun Ahn, Weidi Zhu, Chen Dong, Lingcong Le, Ya-Hsi Hwang, Byung-Jae Kim, Fan Ren, Stephen J. Pearton, Aaron G. Lind, Kevin S. Jones, I. I. Kravchenko, and Ming-Lan Zhang

Citation: *Journal of Vacuum Science & Technology B* **33**, 031210 (2015); doi: 10.1116/1.4918715

View online: <http://dx.doi.org/10.1116/1.4918715>

View Table of Contents: <http://scitation.aip.org/content/avs/journal/jvstb/33/3?ver=pdfcov>

Published by the AVS: Science & Technology of Materials, Interfaces, and Processing

Articles you may be interested in

Study on GaN buffer leakage current in AlGaIn/GaN high electron mobility transistor structures grown by ammonia-molecular beam epitaxy on 100-mm Si(111)

J. Appl. Phys. **117**, 245305 (2015); 10.1063/1.4923035

Influence of stress on structural properties of AlGaIn/GaN high electron mobility transistor layers grown on 150 mm diameter Si (111) substrate

J. Appl. Phys. **113**, 023510 (2013); 10.1063/1.4774288

Effect of buffer structures on AlGaIn/GaN high electron mobility transistor reliability

J. Vac. Sci. Technol. B **31**, 011805 (2013); 10.1116/1.4773060

Effect of buffer layer structure on electrical and structural properties of AlGaIn/GaN high electron mobility transistors

J. Vac. Sci. Technol. B **30**, 011205 (2012); 10.1116/1.3671020

Structural and morphological properties of GaN buffer layers grown by ammonia molecular beam epitaxy on SiC substrates for AlGaIn/GaN high electron mobility transistors

J. Appl. Phys. **103**, 093529 (2008); 10.1063/1.2919163


Instruments for Advanced Science

<p>Contact Hiden Analytical for further details: W www.HidenAnalytical.com E info@hiden.co.uk</p> <p>CLICK TO VIEW our product catalogue</p>	 <p>Gas Analysis</p> <ul style="list-style-type: none"> › dynamic measurement of reaction gas streams › catalysis and thermal analysis › molecular beam studies › dissolved species probes › fermentation, environmental and ecological studies 	 <p>Surface Science</p> <ul style="list-style-type: none"> › UHV TPD › SIMS › end point detection in ion beam etch › elemental imaging - surface mapping 	 <p>Plasma Diagnostics</p> <ul style="list-style-type: none"> › plasma source characterization › etch and deposition process reaction › kinetic studies › analysis of neutral and radical species 	 <p>Vacuum Analysis</p> <ul style="list-style-type: none"> › partial pressure measurement and control of process gases › reactive sputter process control › vacuum diagnostics › vacuum coating process monitoring
---	--	--	--	--

Study of the effects of GaN buffer layer quality on the dc characteristics of AlGaIn/GaN high electron mobility transistors

Shihyun Ahn, Weidi Zhu, Chen Dong, Lingcong Le, Ya-Hsi Hwang, Byung-Jae Kim, and Fan Ren^{a)}

Department of Chemical Engineering, University of Florida, Gainesville, Florida 32611

Stephen J. Pearton, Aaron G. Lind, and Kevin S. Jones

Department of Material Science and Engineering, University of Florida, Gainesville, Florida 32611

I. I. Kravchenko

Center for Nanophase Materials Sciences, Oak Ridge National Laboratory, Oak Ridge, Tennessee 37830

Ming-Lan Zhang

Department of Electronic Science and Technology, Hebei University of Technology, Tianjin 300401, China

(Received 2 March 2015; accepted 9 April 2015; published 21 April 2015)

The effect of buffer layer quality on dc characteristics of AlGaIn/GaN high electron mobility (HEMTs) was studied. AlGaIn/GaN HEMT structures with 2 and 5 μm GaN buffer layers on sapphire substrates from two different vendors with the same Al concentration of AlGaIn were used. The defect densities of HEMT structures with 2 and 5 μm GaN buffer layer were 7×10^9 and $5 \times 10^8 \text{ cm}^{-2}$, respectively, as measured by transmission electron microscopy. There was little difference in drain saturation current or in transfer characteristics in HEMTs on these two types of buffer. However, there was no dispersion observed on the nonpassivated HEMTs with 5 μm GaN buffer layer for gate-lag pulsed measurement at 100 kHz, which was in sharp contrast to the 71% drain current reduction for the HEMT with 2 μm GaN buffer layer. © 2015 American Vacuum Society. [<http://dx.doi.org/10.1116/1.4918715>]

I. INTRODUCTION

Owing to the large bandgaps in the AlGaIn/GaN heterostructure as well as the high electron mobilities and breakdown fields, AlGaIn/GaN high electron mobility transistors (HEMTs) are promising candidates for high power and high current applications in advanced radar systems, inverter units in hybrid electric vehicles, and space and satellite communication networks.^{1–7} AlGaIn/GaN HEMTs are commonly grown on silicon carbide (SiC) or sapphire. It is well established that epitaxial films grown on sapphire or SiC typically have dislocation densities in the order of 10^8 – 10^{10} cm^{-2} due to their thermal coefficient and lattice mismatches.^{8–10} SiC is an excellent substrate candidate for power applications because of its superior thermal conductivity; however, the cost of SiC substrates is high. Therefore, despite its low thermal conductivity, sapphire has an advantage in its lower price and often superior surface quality.

A number of studies have reported that optimizing the parameters of GaN buffer layer growth such as process pressure, precursor flow rate, additional AlN interlayer, and GaN buffer layer thickness can reduce the defect densities, which are caused by lattice mismatch.^{11–13} Also, the thinner GaN buffer layers on SiC have been reported to have higher threading dislocation density in the GaN, but lead to higher off-state breakdown voltages.^{12,13} However, thick GaN buffer layers on sapphire and their impact on dc performance have not been widely studied.

In this paper, the impact of GaN buffer layer quality on dc and gate-lag pulse performance of AlGaIn/GaN HEMTs was investigated. Transmission electron microscopy (TEM) was used to determine the dislocation density in the GaN buffer layer of the HEMT samples. Drain I-Vs, transfer characteristics, and gate pulsed drain I-V characteristics of the HEMTs were measured to establish a correlation between the AlGaIn/GaN HEMTs' dc and gate-pulsed performance and GaN buffer layer quality.

II. EXPERIMENT

AlGaIn/GaN HEMT structures grown by metal organic chemical vapor deposition on sapphire substrates were acquired from two different vendors. Both types of wafers had 24% Al concentration in the AlGaIn barrier layer. One type of wafer had a 5 μm GaN buffer and the other had a 2 μm GaN buffer layer. HEMT fabrication was started with mesa patterning by conventional optical lithography. The mesa-etching was achieved using a unaxis shuttle-lock reactive ion etcher with inductively coupled plasma module (ICP) for device isolation with a Cl_2/Ar plasma. Ohmic metallization of electron-beam evaporated Ti/Al/Ni/Au (25 nm/125 nm/45 nm/100 nm) was patterned by lift-off and subsequently rapid thermally annealed at 850 °C in a flowing N_2 ambient for 45 s. Schottky gates of e-beam evaporated Ni/Au (20 nm/80 nm) with 100 μm width and 1 μm length were obtained by standard lift-off patterning. DC current–voltage (I-V) characteristics were measured using an HP4156 parameter analyzer, and gate-lag pulse measurements were measured using an Agilent 8114A pulse generator.

^{a)}Electronic mail: fren@che.ufl.edu

III. RESULTS AND DISCUSSION

Bright-field cross-sectional TEM (BF-XTEM) was used to quantify the defect density in the HEMT wafers. Figure 1 displays the cross-sectional transmission electron microscopy (XTEM) pictures of AlGaIn/GaN surface for the top layers of (a) HEMT structure with 2 μm GaN buffer layer, (b) HEMT structure with 5 μm GaN buffer layer as well as the GaN/sapphire interface for the (c) HEMT structure with 2 μm GaN buffer layer, and (d) HEMT structure with 5 μm GaN buffer layer. Dislocations are seen to originate near the GaN/sapphire interface and propagate up through the AlGaIn/GaN interface to the surface of both HEMT wafers. However, it is clear that the HEMT structure with 2 μm GaN buffer layer exhibited a much higher defect density. The defect density near the surface for the two substrates was calculated from XTEM taken along the length of the TEM lamella based on the thickness measured during lamella formation with a focused ion beam. In the case of the 5 μm GaN buffer layer substrate, the measured defect density was $5 \times 10^8 \text{ cm}^{-2}$, while an order of magnitude higher measured defect density of $7 \times 10^9 \text{ cm}^{-2}$ was observed for the 2 μm GaN buffer layer sample.

Although the HEMT wafer with 5 μm GaN buffer had one order less defect density, this wafer was under a high strain. As shown in Fig. 2, the HEMT wafer with 5 μm GaN buffer layer was significantly bowed. A height difference of 70 μm across the 2 in. wafer was measured with a much smaller radius of curvature of 5 m. On the contrary, the HEMT wafer with 2 μm GaN buffer layer was flat and the wafer height difference across 3 in. wafer was around 21.25 μm with a radius of curvature of 45 m. These results indicate that the HEMT wafer with 5 μm GaN buffer layer was highly strained by lower defect density.

Figure 3 shows the drain current–voltage (I–V) characteristics of HEMTs fabricated on the different thickness of

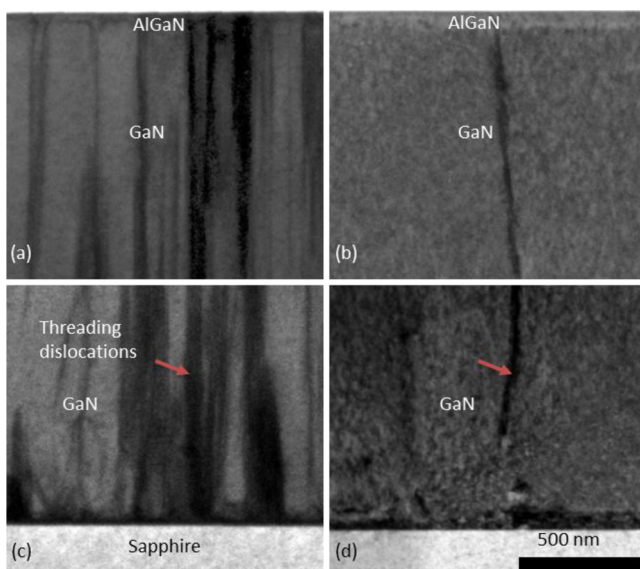


FIG. 1. (Color online) BF-XTEM showing the AlGaIn/GaN interface for the (a) 2 μm GaN and (b) 5 μm GaN substrates and the GaN/sapphire interface for the (c) 2 μm GaN and (d) 5 μm GaN substrates.

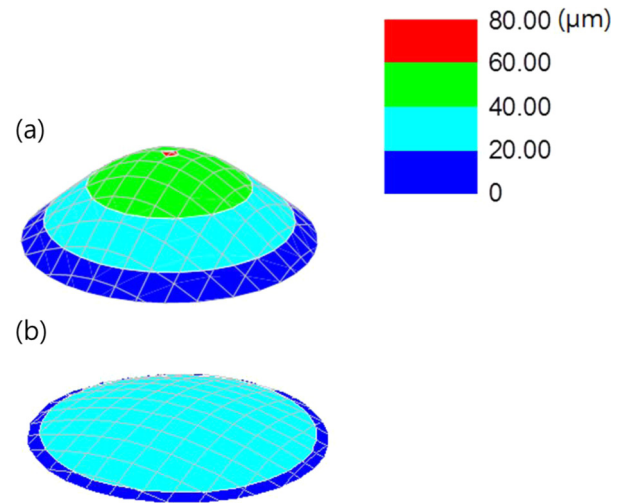


FIG. 2. (Color online) Schematics of wafer bowing for HEMT wafer with (a) 5 μm and (b) 2 μm GaN buffer layer.

buffer layers. The HEMTs were measured by sweeping V_{DS} from 0 to 5 V, while V_G started from +1 V with a step of -1 V till reaching pinch-off. There was a little difference in the saturation current observed at $V_{DS} = +5$ V. Transfer characteristics of HEMTs fabricated on different buffer layers were measured at $V_{DS} = +5$ V and V_g was swept from -5 to 0 V, as illustrated in Fig. 4. The thicker buffer GaN layer HEMTs showed marginally higher drain current at $V_G = 0$ V than the thinner GaN layer HEMTs, with current densities of 312 and 300 mA/mm, respectively. The peak transconductance for 5 μm GaN buffer layer HEMTs was 119 mS/mm and for the thinner GaN layer HEMTs was 112 mS/mm, showing only a slightly higher value for the thicker GaN layer HEMT. Using the linear region of the drain I–V curve, the mobility and carrier concentration were calculated using a charge control model.^{14,15} The calculated mobility and carrier concentration for thicker GaN layer HEMTs were 989 $\text{cm}^2/\text{V s}$ and $8.45 \times 10^{12} \text{ cm}^{-2}$ and for thinner GaN layer HEMTs were 907 $\text{cm}^2/\text{V s}$ and $8.63 \times 10^{12} \text{ cm}^{-2}$. These similarities in their dc characteristics suggest that the

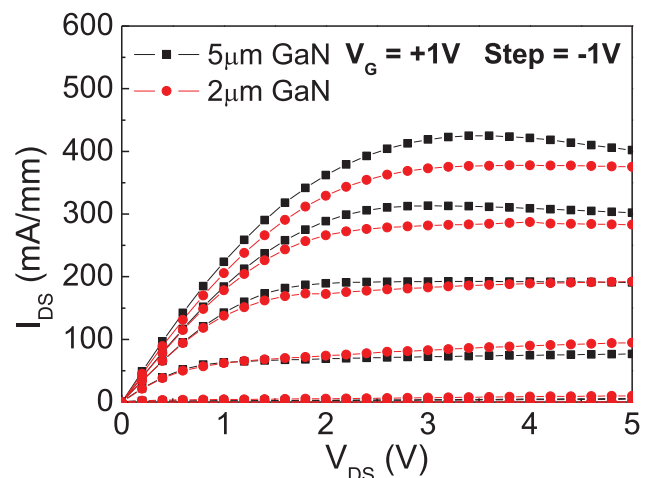


FIG. 3. (Color online) Drain I–Vs of HEMTs fabricated on different GaN buffer layer structures.

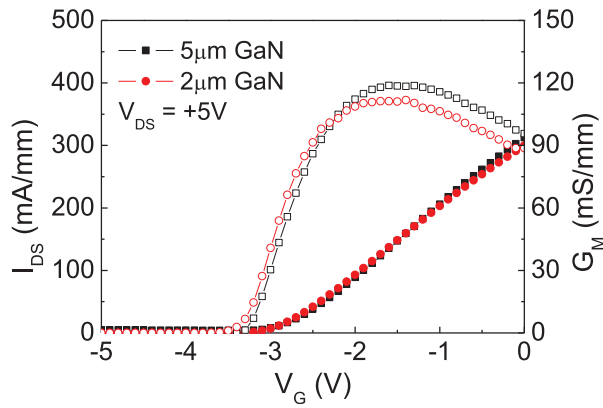


FIG. 4. (Color online) Transfer characteristics of HEMTs fabricated on different GaN buffer layer structures.

defect density in GaN buffer layer has a minimal influence on HEMT dc performance over this range of buffer thicknesses.

Furthermore, gate-lag pulse measurements were applied to evaluate the effect of the different GaN buffer layers on material electrical quality. In this method, the drain current (I_{DS}) was recorded while gate voltage (V_G) was pulsed. The

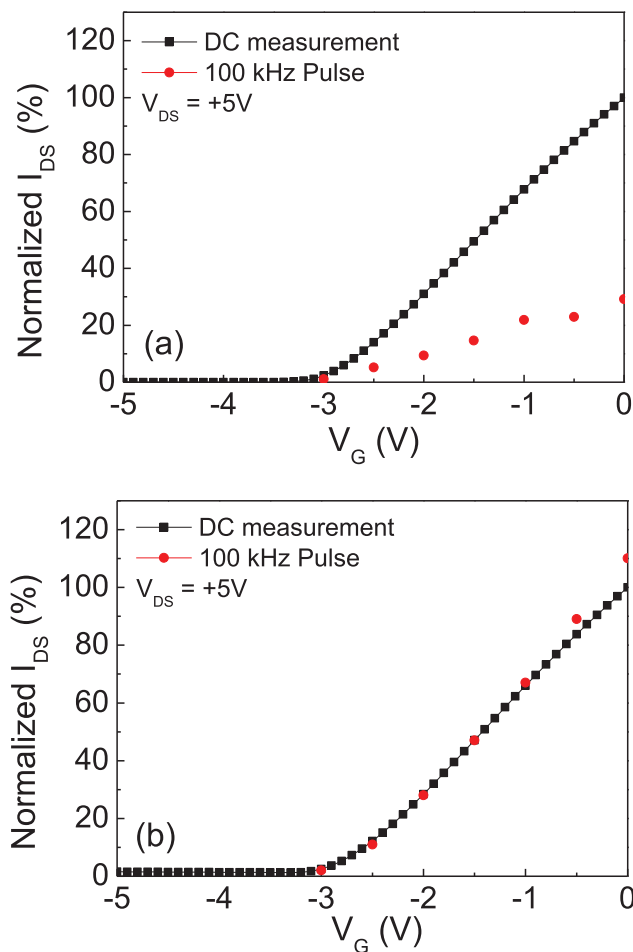


FIG. 5. (Color online) (a) Gate-lag pulsed measurements on HEMTs fabricated with a $2\ \mu\text{m}$ GaN buffer layer. (b) Gate-lag pulsed measurements on HEMTs fabricated with a $5\ \mu\text{m}$ GaN buffer layer.

normalized drain current–gate voltage (V_G) and pulsed measurements are shown in Fig. 5. V_G was pulsed from $-5\ \text{V}$ to the voltage indicated on the x-axis in Fig. 5 at 100 kHz frequency with 10% duty cycle while V_{DS} was kept $+5\ \text{V}$. As shown in Fig. 5(a), a dramatic reduction of drain current was observed during the gate-pulsed measurement for the HEMT with $2\ \mu\text{m}$ GaN buffer layer. When the gate was pulsed at a fixed drain voltage, some of the surface traps become charged by trapping hot electrons.¹⁵ If the gate is pulsed above a certain high frequency, the traps do not have enough time to detrapp. Those charged traps acted as a virtual gate and formed an additional depletion region between gate and drain electrodes, and reduced the drain current. However, there was no drain current reduction during the gate pulsed measurement for the HEMT with $5\ \mu\text{m}$ GaN buffer layers. On the other hand, there was 71% of drain current reduction in the gate pulsed measurement for the HEMT with $2\ \mu\text{m}$ GaN buffer layer at $V_G = 0\ \text{V}$. This indicates that the excess number of defects in the thinner GaN buffer layer influenced the generation of surface trap and induced drain current collapse at high frequency operation.

IV. CONCLUSIONS

The effects of defect density on HEMT dc and rf performance were studied. HEMTs were fabricated on 2 and $5\ \mu\text{m}$ of GaN buffer layers with the same composition of active layers. TEM showed that the thinner GaN layers had an order of magnitude higher defect densities. HEMTs on thicker GaN buffer layers showed negligible difference in the drain I-V characteristics and showed a 6% higher value in peak transconductance. Significant reduction in pulse measurements was observed on thinner GaN layer HEMTs. These results suggest that the defects created in GaN buffer layer do not largely influence device dc performance but are closely related to high frequency performance.

ACKNOWLEDGMENTS

The work performed at UF was supported by an U.S. DOD HDTRA Grant No. 1-11-1-0020 monitored by James Reed and a NSF Grant No. ECCS-1445720 monitored by John Zavada. The authors would like to thank Ajit Paranjpe for materials support. A portion of this research was conducted at the Center for Nanophase Materials Sciences, which is a DOE Office of Science User Facility.

¹P. Srivastava *et al.*, *IEEE Electron Device Lett.* **32**, 30 (2011).

²H. Sun, A. Alt, H. Benedickter, and C. Bolognesi, *IEEE Electron Device Lett.* **45**, 376 (2009).

³L. Bin and T. Palacios, *IEEE Electron Device Lett.* **31**, 951 (2010).

⁴M. Ochiai, M. Akitai, Y. Ohno, S. Kishimoto, K. Maezawa, and T. Mizutani, *Jpn. J. Appl. Phys., Part 1* **42**, 2278 (2003).

⁵T. Hashizume, S. Anantathanasarn, N. Negoro, E. Sano, H. Hasegawa, K. Kumakura, and T. Makimoto, *Jpn. J. Appl. Phys., Part 2* **43**, L777 (2004).

⁶M. Kanamura, T. Ohki, T. Kikkawa, K. Imanishi, T. Imada, A. Yamada, and N. Hara, *IEEE Electron Device Lett.* **31**, 189 (2010).

⁷Y. Irokawa *et al.*, *Appl. Phys. Lett.* **84**, 2919 (2004).

⁸M. A. Khan, X. Hu, A. Tarakji, G. Simin, J. Yang, R. Gaska, and M. S. Shur, *Appl. Phys. Lett.* **77**, 1339 (2000).

⁹A. Hinoki *et al.*, *Appl. Phys. Express.* **1**, 011103 (2008).

- ¹⁰A. E. Wickenden, D. D. Koleske, R. L. Henry, M. E. Twigg, and M. Fatemi, *J. Cryst. Growth* **260**, 54 (2004).
- ¹¹Z. Bougrioua, I. Moerman, L. Nistor, B. Van Daele, E. Monroy, T. Palacios, F. Calle, and M. Leroux, *Phys. Status Solidi A* **195**, 93 (2003).
- ¹²A. Hinoki, S. Kamiya, T. Tsuchiya, T. Yamada, J. Kikawa, T. Araki, A. Suzuki, and Y. Nanishi, *Phys. Status Solidi C* **4**, 2728 (2007).
- ¹³L. Liu, C. F. Lo, Y. Xi, F. Ren, S. J. Pearton, O. Laboutin, Y. Cao, W. Johnson, and I. I. Kravchenko, *J. Vac. Sci. Technol., B* **31**, 011805 (2013).
- ¹⁴Y. Zhang, I. P. Smorchkova, C. R. Elass, S. Keller, J. P. Ibbertson, S. DenBaars, U. K. Mishra, and J. Singh, *J. Appl. Phys.* **87**, 7981 (2000).
- ¹⁵R. Vetury, N. Q. Zhang, S. Keller, and U. K. Mishra, *IEEE Trans. Electron Devices* **48**, 560 (2001).